ChemComm

COMMUNICATION

View Article Online
View Journal

Open Access Article. Published on 14 August 2025. Downloaded on 8/26/2025 7:26:27 AM.
This article is licensed under a Creative Commons Attribution-NonCommercial 3.0 Unported Licence.

Check for updates

Cite this: DOI: 10.1039/d5cc04263a

Synthesis of a highly strained deep cavitand

M. Saeed Mirzaei,†[a] Saber Mirzaei, †[ab] Hormoz Khosravi[a] and Raúl Hernández Sánchez *[abc]

Received 30th July 2025,
Accepted 13th August 2025

DOI: 10.1039/d5cc04263a

rsc.li/chemcomm

Access to highly strained molecules remains a challenge. We report the synthesis of a bench-stable and highly strained (~135 kcal mol^{-1}) deep cavitand (1). Synthesis of 1 follows a two-step protocol from known starting materials. The rigid structure of 1 contains four arch-shaped biphenylenes with a large cavity (~500 Å^3) to host fullerenes.

Challenging Hückel's rule to discover new phenomena by bending aromatic systems from their stable planar geometry is an ongoing scientific endeavor.[1] Although the discovery of fullerenes brought to light spherical aromaticity,[2] the synthesis of discrete compounds with bent aromatic systems was considered a major challenge.[3] Anthracene dimers and [*n*]cyclo-*para*-phenylacetylenes were the first molecular species with radial aromaticity.[4,5] Years later, the synthesis of [*n*]cyclo-*para*-phenylenes ([*n*]CPPs) was put forward by Jasti *et al.*[6] To date, several methods have been developed to build highly-strained and contorted nanohoops[7] revealing novel applications.[8] The smallest [*n*]CPP reported to date is [5]CPP,[9,10] which has a strain energy (SE) of ~120 kcal mol^{-1} (Fig. 1a).[11] Other strained molecules close in SE to [5]CPP are known in the literature.[12–15] Further up on the SE scale are Stępień's carbazole-based bowls (Fig. 1b),[16] and Kayahara and Yamago's doubly-annulated [10]cycloparaphenylene (Fig. 1c),[17] with 138/144 and ~150 kcal mol^{-1} of strain, respectively. Higher up on strain is a triple hoop compound with 24 aromatic rings at ~153 kcal mol^{-1} reported by Tian, Ye, and Sun (Fig. 1d).[18] A similar, yet less strained, species was reported by Jasti *et al.*[19] Last, and to the best of our knowledge, Tanaka's carbon cage (163 kcal mol^{-1}, Fig. 1e)[20] and Wang's molecular bowl (~164 kcal mol^{-1}, Fig. 1f)[21] display the largest SEs known to date. Here, we report **1** – a highly strained deep cavitand with SE of ~135 kcal mol^{-1} and unusually high host:guest binding affinity for fullerenes (Fig. 1g).

Our group and others have developed a synthetic approach towards contorted macrocycles based on macrocyclic arene species, *e.g.*, resorcin[4]arenes.[22–25] In our work, the resulting tubular species develop a sizable strain in the last synthetic step reaching values of *ca.* 90 kcal mol^{-1} at poor isolated yields of <1–3%. We hypothesized that low yields could be overcome by moving away from intermolecular reactions in exchange for intramolecular couplings. The success of this approach was demonstrated recently with the synthesis of **1m**,[26] a non-strained analogue of **1**, and has also been exemplified by others in recent reports.[27] Following an intramolecular Ni-mediated homocoupling reaction, and comparing it to our previous reports employing intermolecular cross couplings, led us to improve our yields by 20-fold in the strain-forming step.

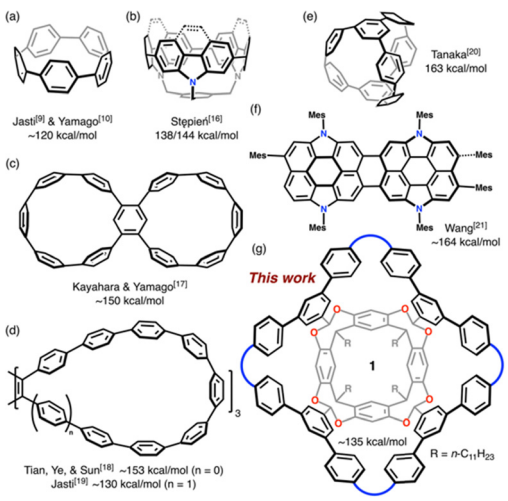

Fig. 1 Highly strained conjugated aromatic structures. (a)–(f) Previous examples reported in the literature. (g) This work, deep cavitand **1**. Values shown correspond to the DFT-calculated strain energies. SE in (f) was calculated using StrainViz.[29]

[a] *Department of Chemistry, Rice University, 6100 Main St., Houston, TX 77005, USA. E-mail: raulhs@rice.edu*
[b] *Department of Chemistry, University of Pittsburgh, 219 Parkman Ave., Pittsburgh, PA 15260, USA*
[c] *Rice Advanced Materials Institute, Rice Sustainability Institute, and Rice WaTER Institute, Rice University, Houston, TX 77005, USA*
† These authors contributed equally.

Open Access Article. Published on 14 August 2025. Downloaded on 8/26/2025 7:26:27 AM. This article is licensed under a Creative Commons Attribution-NonCommercial 3.0 Unported Licence.

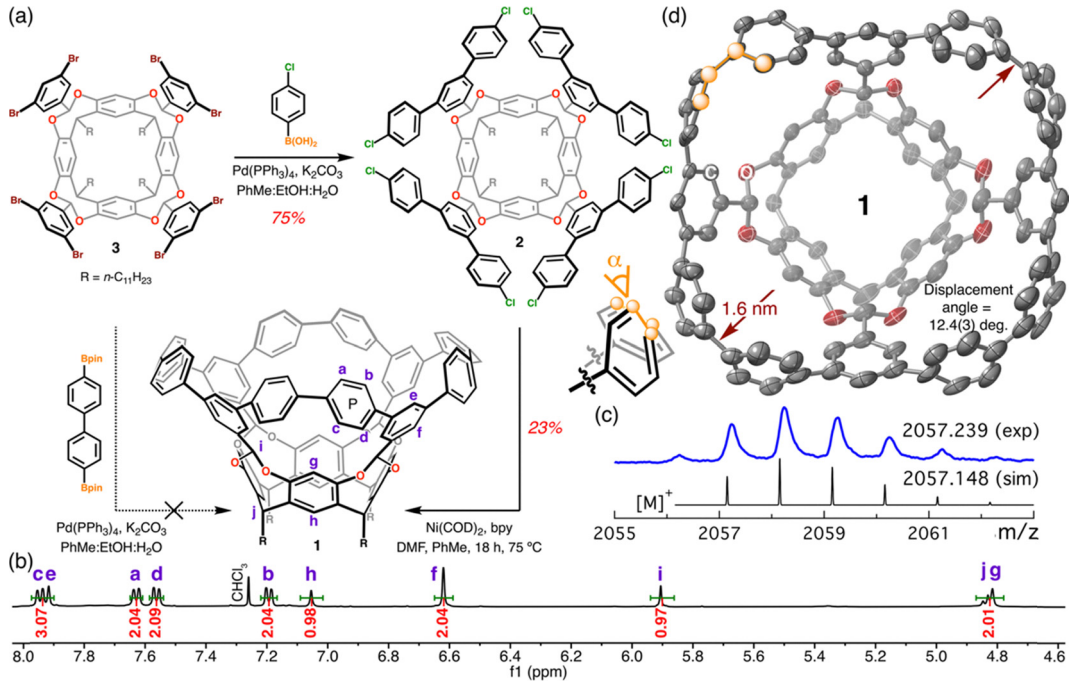

Fig. 2 (a) Templated synthesis of **1** indicating the intra- and intermolecular approach. (b) ^{1}H NMR of **1** in $CDCl_3$ collected at room temperature. Integration is provided considering one-fourth of **1**. (c) Experimental MALDI MS molecular ion peaks of **1** (blue trace). Black trace represents the simulated $[M]^+$ isotopic distribution. (d) Molecular crystal structure of **1** obtained at 100 K. Thermal ellipsoids are set at 50% probability level. The C and O atoms are colored grey and red, respectively. The H atoms and R groups are omitted for clarity. Inset: Chemdraw drawing indicating the torsional angle α. Maroon arrows indicate the distance of 1.6 nm from the midpoint of one distorted biphenyl to the opposing one.

The synthesis of **1** – a highly strained deep-cavity molecular container – consists on derivatizing **3**[28] through a Suzuki – Miyaura cross coupling reaction with *para*-chlorophenyl boronic acid resulting in compound **2** in 75% yield (Fig. 2a). The yield obtained for **2** is remarkable as eight C–C bonds are formed. Subsequently, a Ni-mediated Yamamoto cross coupling leads to **1** as a white solid in 23% yield. In comparison, the intermolecular Suzuki–Miyaura cross coupling between **3** and 4,4′-biphenyldiboronic acid bis(pinacol) ester does not produce **1** in detectable quantities (Fig. 2a). Using *meta*-chlorophenyl boronic acid in this reaction sequence leads to **1m**, which is substantially less rigid than **1** (SE = ∼9 kcal mol^{-1}, SI).[26]

Analysis of **2** *via* ^{1}H NMR displays six aromatic resonances indicating an ideal C_4-symmetric structure in solution (Fig. S1). Formation of **1** results in eight aromatic resonances suggesting that a species of similar symmetry to **2** is formed yet with additional intricacies (Fig. 2b). This observation led us to propose that phenylene ring "P" cannot freely rotate making resonances "a" and "c" no longer equivalent as in **2**; similarly, "b" and "d" are unique resonances in **1**. COSY and NOESY NMR supports the assignment of **1** (Fig. S5–S7). Note that MALDI-MS of **1** match perfectly the simulated pattern of its cationic molecular ion peak, $[M]^+$ (Fig. 2c). Variable temperature ^{1}H NMR of **1** in 1,1,2,2-tetrachloroethane-d_2 (TeCA-d_2) from 25 to 115 °C showcases non-coalescing resonances confirming the rigid nature of "P" (Fig. S8). DFT calculations indicate a rotational barrier of ∼25 kcal mol^{-1} for "P", similar to other rigid systems.[30]

The top-rim of **1** contains twelve phenylenes connected in a unique and alternating 2 : 1 *para* : *meta* fashion. We did not observe decomposition, color change, or the formation of new products during the purification of **1** using silica gel or after prolonged time on the benchtop, as shown through MALDI-MS and ^{1}H NMR. In contrast, other strained systems are known to decompose over time.[9,16] We grew colorless crystals by slow diffusion of MeCN into a chlorobenzene solution of **1**. The structure of **1** is shown in Fig. 2d providing a clear view of the biphenyl contortion with an average displacement angle of 12.4(3) degrees, similar to [6]CPP (12.6 deg.),[12] and a torsional angle (α) of 10(3) deg. which is smaller than [5]CPP and [6]CPP at 12(2)[9] and 26.4(7) deg.,[31] respectively. Last, biphenyl contortion produces a large and unexpected shielding of the "g" resonance as it shifts from 6.74 ppm in **2** to 4.82 ppm in **1**, suggesting an anisotropic effect is induced by the biphenyl moieties despite the distance of ∼5.2 Å to the centroid of "P".

The SE of **1′** (R = Me) was calculated considering two different homodesmotic reactions (Fig. S9) and six different DFT functionals (Table S2). From all twelve calculations, the SE of **1′** ranges from 128 to 147 kcal mol^{-1}. Data obtained using B3LYP/6-31G(d) provides a SE for **1′** of ∼135 kcal mol^{-1}, which allow us to compare with literature values. For instance, the SE of [6]CPP is 97 kcal mol^{-1} making an average strain of ∼16 kcal mol^{-1} per aryl ring.[12] In comparison, the same metric for **1′** is ∼17 kcal mol^{-1} considering only the aromatic rings within the four distorted biphenyls. In stark contrast, the *meta*-connected species **1m′** has a minor contortion of ∼9 kcal mol^{-1} of SE or 1.1 kcal mol^{-1} per aryl ring in the connecting biphenyls (Fig. S10).

 This journal is © The Royal Society of Chemistry 2025

Open Access Article. Published on 14 August 2025. Downloaded on 8/26/2025 7:26:27 AM. This article is licensed under a Creative Commons Attribution-NonCommercial 3.0 Unported Licence.

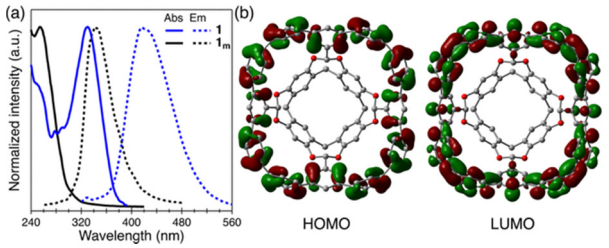

Fig. 3 (a) UV-vis absorption and emission spectra of **1** (blue traces) and **1m** (black traces) collected in CH_2Cl_2 at room temperature. (b) HOMO and LUMO density plots of **1** (±0.02 au).

We examined the electronic properties of **1** *via* UV-vis absorption, fluorescence emission, and supported our findings through TD-DFT calculations. Its lowest energy absorption band is observed at λ_{max} of 331 nm in CH_2Cl_2 at room temperature, which is red shifted by ~80 nm relative to **1m** (Fig. 3a). A fluorescence red shift of 81 nm is seen between **1** (λ_{em} = 425 nm) and **1m** (λ_{em} = 344 nm). A visual comparison of the fluorescence shift is shown in Fig. S11. We attribute these differences to greater π conjugation in **1**. The fluorescence quantum yield (ϕ_f) of **1** is 0.06 as determined by the relative method described by Williams *et al.*[32] using anthracene as standard. For reference, [5]CPP and [6]CPP are not emissive.[9,10,31] The smallest member in the [*n*]CPP family with measurable fluorescence is [7]CPP with ϕ_f of 0.0007.[33] Based on TD-DFT calculations, we attribute the major absorption band in **1** at λ_{max} of 331 nm to H → L + 1 and H → L + 2 transitions, where H and L stands for HOMO and LUMO, respectively. The H → L transition is forbidden (Table S3), similar to [*n*]CPPs.[11] Despite heavy contortion of **1**, its HOMO displays an overall benzenoid structure distributed over all twelve phenylenes atop the resorcin[4]arene (Fig. 3b). DFT results on **1′** indicate a HOMO–LUMO gap of 3.99 eV, while the unstrained analogue **1m′** has a larger gap of 4.73 eV, which is similar to the trend in [*n*]CPPs where the HOMO–LUMO gap increases as strain decreases.[34]

The rigidity of **1** produces a large shape-persistent cavity. The crystal structure of **1** showcases cofacial packing producing a shared cavity space for twelve MeCN molecules. Using the molecular volume of MeCN (87.8 Å^3)[35] and the void space calculator of Olex2,[36] we determine the size of this cavity to be between 465 and 527 Å^3 (Fig. S13). Molecular containers display cavities from ~90 to ~400 Å^3,[37–44] except for a recent report describing a species with a cavity of ~800 Å^3.[45] Despite these reports, hosts with large pseudospherical cavities are rare.[46]

We hypothesized **1** can host fullerenes, similar to **1m**.[26] ^{1}H NMR titration experiments showed that addition of C_{60} or C_{70} to **1** generates a new set of resonances that co-exist with those of free host **1** (Fig. 4) suggesting a large association constant (K_a) for adduct formation. No further spectral changes are observed after addition of 1 equivalent of C_{60}. The benzal proton in **1**, resonance "i", experiences an upfield shift from 5.96 to 5.87 ppm and points directly at the π surface of C_{60}. Computational data demonstrates that shielding effects occur above the hexagonal rings in C_{60} and C_{70}, and deshielding over the pentagons.[47] We conclude that on average the benzal proton in $C_{60} \subset$ **1** points at hexagons in C_{60}. Titration of C_{70} to **1** also results

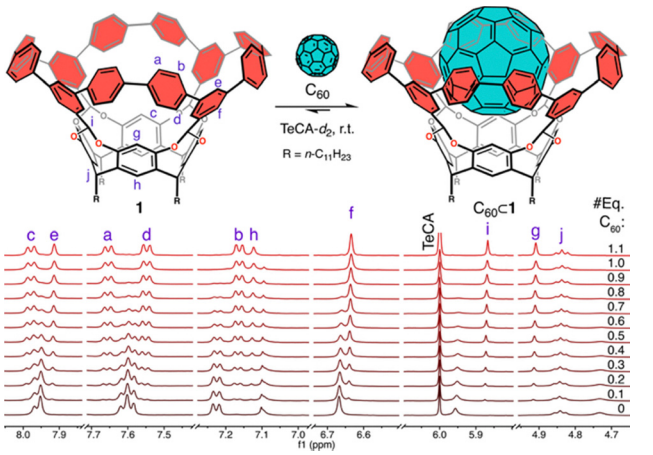

Fig. 4 ^{1}H NMR titration of C_{60} into **1** in TeCA-d_2 at room temperature.

in an upfield shift of the benzal proton to 5.87 ppm (Fig. S15); thus, nesting of C_{60} and C_{70} within **1** occurs in a similar fashion. Last, the diffusion properties of **1** and its fullerene adducts were probed *via* DOSY NMR. We expect **1** to have a larger diffusion coefficient (D) than its fullerene adducts (D = 1.34(1) × 10^{-10} m^2 s^{-1}, Fig. S16); however, it was surprising to find that adducts $C_{60} \subset$ **1** and $C_{70} \subset$ **1** also differ in its D from 1.26(1) × 10^{-10} to 1.10(1) × 10^{-10} m^2 s^{-1} (Fig. S17 and S18), respectively.

Binding data for fullerene ⊂ **1** was obtained from fluorescence quenching experiments. Titration of C_{60}/C_{70} into **1** were performed in TeCA (Fig. S19 and S20). Fitting of the data using Bindfit[48] reveals K_as of 5.7(13) × 10^5 and 5.5(19) × 10^5 M^{-1} for $C_{60} \subset$ **1** and $C_{70} \subset$ **1**, respectively, which are lower than the non-strained analogues $C_{60} \subset$ **1m** and $C_{70} \subset$ **1m**.[26] These K_as are medium-to-large,[49] with the exception of a few examples displaying higher binding affinities.[50,51] Last, we calculated the non-covalent interaction surface through the Hirshfeld partition of molecular density (IGMH) to visualize the nesting between C_{60} or C_{70} and **1**.[52] The IGMH isosurface shows the interaction between the contorted biphenyls, π contacts, and the benzal protons of **1** with fullerene's π surface (Fig. S21).

In summary, we developed the synthesis of **1** – a highly strained deep cavitand built atop an alkyl resorcin[4]arene scaffold. The final product contains four highly contorted arch-shaped biphenylenes. The overall strain energy of **1** is ~135 kcal mol^{-1}. The rigid structure of **1** produces a large internal void space enough to accommodate fullerenes. Our approach will allow the synthesis of other highly strained molecules pushing the known boundaries in contorted aromatic chemistry.

This research was partially supported by NSF CAREER CHE-2302628 and funds by Rice University. R. H. S. acknowledges the support of the Robert A. Welch Foundation Young Investigator Award and Welch Foundation grant C-2142-20230405. We thank Dr Christopher L. Pennington for assistance with HRMS. S. M. acknowledges the support from the Dietrich School of Arts & Sciences Graduate Fellowship and the Andrew Mellon Predoctoral Fellowship. We thank the support from the CRC and instrumentation made available through SEA at Rice University.

Open Access Article. Published on 14 August 2025. Downloaded on 8/26/2025 7:26:27 AM. This article is licensed under a Creative Commons Attribution-NonCommercial 3.0 Unported Licence.

Conflicts of interest

There are no conflicts to declare.

Data availability

All the supporting data associated with this work are available in the SI. The SI includes general experimental procedures, characterization details, crystallographic information, ^{1}H NMR, ^{13}C NMR, UV-vis, and fluorescence spectra of all compounds (PDF). See DOI: **https://doi.org/10.1039/d5cc04263a**

CCDC 2393731 contains the supplementary crystallographic data for this paper.[53]

Notes and references

1 M. A. Majewski and M. Stepien, *Angew. Chem., Int. Ed.*, 2019, **58**, 86–116.
2 M. Bühl and A. Hirsch, *Chem. Rev.*, 2001, **101**, 1153–1184.
3 P. R. Ashton, N. S. Isaacs, F. H. Kohnke, A. M. Z. Slawin, C. M. Spencer, J. F. Stoddart and D. J. Williams, *Angew. Chem., Int. Ed. Engl.*, 1988, **27**, 966–969.
4 S. Kammermeier, P. G. Jones and R. Herges, *Angew. Chem., Int. Ed. Engl.*, 1996, **35**, 2669–2671.
5 T. Kawase, H. R. Darabi and M. Oda, *Angew. Chem., Int. Ed. Engl.*, 1996, **35**, 2664–2666.
6 R. Jasti, J. Bhattacharjee, J. B. Neaton and C. R. Bertozzi, *J. Am. Chem. Soc.*, 2008, **130**, 17646–17647.
7 S. Mirzaei, E. Castro and R. Hernández Sánchez, *Chem. – Eur. J.*, 2021, **27**, 8642–8655.
8 E. J. Leonhardt and R. Jasti, *Nat. Rev. Chem.*, 2019, **3**, 672–686.
9 P. J. Evans, E. R. Darzi and R. Jasti, *Nat. Chem.*, 2014, **6**, 404–408.
10 E. Kayahara, V. K. Patel and S. Yamago, *J. Am. Chem. Soc.*, 2014, **136**, 2284–2287.
11 T. Iwamoto, Y. Watanabe, Y. Sakamoto, T. Suzuki and S. Yamago, *J. Am. Chem. Soc.*, 2011, **133**, 8354–8361.
12 E. R. Darzi and R. Jasti, *Chem. Soc. Rev.*, 2015, **44**, 6401–6410.
13 L.-H. Wang, N. Hayase, H. Sugiyama, J. Nogami, H. Uekusa and K. Tanaka, *Angew. Chem., Int. Ed.*, 2020, **59**, 17951–17957.
14 X. Zhang, H. Shi, G. Zhuang, S. Wang, J. Wang, S. Yang, X. Shao and P. Du, *Angew. Chem., Int. Ed.*, 2021, **60**, 17368–17372.
15 C. Chi, Y. Han, S. Dong, J. Shao and W. Fan, *Angew. Chem., Int. Ed.*, 2021, **60**, 2658–2662.
16 D. Myśliwiec, M. Kondratowicz, T. Lis, P. J. Chmielewski and M. Stępień, *J. Am. Chem. Soc.*, 2015, **137**, 1643–1649.
17 L. Sun, E. Kayahara, T. Nishinaga, M. Ball, D. Paley, C. Nuckolls and S. Yamago, *Bull. Chem. Soc. Jpn.*, 2024, **97**, uoad011.
18 Q. Zhou, Z. Xu, K. Li, X. Tian, L. Ye and Z. Sun, *Chem. – Asian J.*, 2024, **19**, e202301131.
19 T. D. Clayton, J. M. Fehr, T. W. Price, L. N. Zakharov and R. Jasti, *J. Am. Chem. Soc.*, 2024, **146**, 30607–30614.
20 N. Hayase, J. Nogami, Y. Shibata and K. Tanaka, *Angew. Chem., Int. Ed.*, 2019, **58**, 9439–9442.
21 W. Zhang, Y. Ding, S. Yu, J. Lyu, J. Yu, J. Li, X. Zhao, L. Feng, J. Wang, Z. Zhou and Q. Wang, *Angew. Chem., Int. Ed.*, 2025, **64**, e202425355.
22 E. André, B. Boutonnet, P. Charles, C. Martini, J.-M. Aguiar-Hualde, S. Latil, V. Guérineau, K. Hammad, P. Ray, R. Guillot and V. Huc, *Chem. – Eur. J.*, 2016, **22**, 3105–3114.
23 S. Mirzaei, E. Castro and R. Hernández Sánchez, *Chem. Sci.*, 2020, **11**, 8089–8094.
24 E. Castro, S. Mirzaei and R. Hernández Sánchez, *Org. Lett.*, 2021, **23**, 87–92.
25 A. Nasser Moussa Bamba, A. Ben Saida, I. Abdellah, S. Latil, V. Guérineau, J.-F. Gallard and V. Huc, *Eur. J. Org. Chem.*, 2024, e202400485.
26 S. Mirzaei, H. Khosravi, X. Hu, M. S. Mirzaei, V. M. E. Castro, X. Wang, N. A. Figueroa, T. Chang, Y.-P. Chen, G. P. Ríos, N. I. Gonzalez-Pech, Y.-S. Chen and R. Hernández Sánchez, *Angew. Chem., Int. Ed.*, 2025, **64**, e202505083.
27 Z. Sun, K. Ikemoto, T. M. Fukunaga, T. Koretsune, R. Arita, S. Sato and H. Isobe, *Science*, 2019, **363**, 151–155.
28 K. Srinivasan and B. C. Gibb, *Org. Lett.*, 2007, **9**, 745–748.
29 C. E. Colwell, T. W. Price, T. Stauch and R. Jasti, *Chem. Sci.*, 2020, **11**, 3923–3930.
30 Z. Sun, T. Suenaga, P. Sarkar, S. Sato, M. Kotani and H. Isobe, *Proc. Natl. Acad. Sci. U. S. A.*, 2016, **113**, 8109.
31 J. Xia and R. Jasti, *Angew. Chem., Int. Ed.*, 2012, **51**, 2474–2476.
32 A. T. R. Williams, S. A. Winfield and J. N. Miller, *Analyst*, 1983, **108**, 1067–1071.
33 T. J. Sisto, M. R. Golder, E. S. Hirst and R. Jasti, *J. Am. Chem. Soc.*, 2011, **133**, 15800–15802.
34 K. Kanai, T. Inoue, T. Furuichi, K. Shinoda, T. Iwahashi and Y. Ouchi, *Phys. Chem. Chem. Phys.*, 2021, **23**, 8361–8367.
35 M. Sakurai, *J. Chem. Eng. Data*, 1992, **37**, 358–362.
36 O. V. Dolomanov, L. J. Bourhis, R. J. Gildea, J. A. K. Howard and H. Puschmann, *J. Appl. Cryst.*, 2009, **42**, 339–341.
37 J. R. Moran, S. Karbach and D. J. Cram, *J. Am. Chem. Soc.*, 1982, **104**, 5826–5828.
38 D. M. Rudkevich, G. Hilmersson and J. Rebek, *J. Am. Chem. Soc.*, 1997, **119**, 9911–9912.
39 H. Xi and C. L. D. Gibb, *Chem. Commun.*, 1998, 1743–1744.
40 F. C. Tucci, D. M. Rudkevich and J. Rebek, *J. Org. Chem.*, 1999, **64**, 4555–4559.
41 E. Botana, K. Nättinen, P. Prados, K. Rissanen and J. de Mendoza, *Org. Lett.*, 2004, **6**, 1091–1094.
42 I. Pochorovski, C. Boudon, J.-P. Gisselbrecht, M.-O. Ebert, W. B. Schweizer and F. Diederich, *Angew. Chem., Int. Ed.*, 2012, **51**, 262–266.
43 F. Bertani, N. Riboni, F. Bianchi, G. Brancatelli, E. S. Sterner, R. Pinalli, S. Geremia, T. M. Swager and E. Dalcanale, *Chem. – Eur. J.*, 2016, **22**, 3312–3319.
44 J. Pfeuffer-Rooschüz, L. Schmid, A. Prescimone and K. Tiefenbacher, *JACS Au*, 2021, **1**, 1885–1891.
45 J. Pfeuffer-Rooschüz, S. Heim, A. Prescimone and K. Tiefenbacher, *Angew. Chem., Int. Ed.*, 2022, **61**, e202209885.
46 B. Chen, J. J. Holstein, S. Horiuchi, W. G. Hiller and G. H. Clever, *J. Am. Chem. Soc.*, 2019, **141**, 8907–8913.
47 E. Kleinpeter, S. Klod and A. Koch, *J. Org. Chem.*, 2008, **73**, 1498–1507.
48 **https://supramolecular.org**.
49 X. Chang, Y. Xu and M. von Delius, *Chem. Soc. Rev.*, 2024, **53** 47–83.
50 H. Isobe, S. Hitosugi, T. Yamasakia and R. Iizukaa, *Chem. Sci.*, 2013, **4**, 1293–1297.
51 M. Takeda, S. Hiroto, H. Yokoi, S. Lee, D. Kim and H. Shinokubo, *J. Am. Chem. Soc.*, 2018, **140**, 6336–6342.
52 T. Lu and Q. Chen, *J. Comput. Chem.*, 2022, **43**, 539–555.
53 M. S. Mirzaei, S. Mirzaei, H. Khosravi, R. Hernández Sánchez, CCDC 2393731: Experimental Crystal Structure Determination, 2024, DOI: **10.5517/ccdc.csd.cc2lbw4z**.

 This journal is © The Royal Society of Chemistry 2025